DOI: 10.1021/ma100501j

Macromolecules
ARTICLE

Hydrogen-Bonded Aggregates of Oligoaramide−Poly(ethylene glycol) Block Copolymers

Anne Bohle,[†] Gunther Brunklaus,[†] Michael R. Hansen,[†] Tobias W. Schleuss,[‡] Andreas F. M. Kilbinger,[‡] Jens Seltmann,[§] and Hans W. Spiess*,[†]

[†]*Max Planck Institute for Polymer Research, Ackermannweg 10, D-55128 Mainz, Germany,* [‡]*Johannes Gutenberg-Universität Mainz, Duesbergweg 10-14, D-55099 Mainz, Germany, and* [§]*Technische Universität Chemnitz, Strasse der Nation 62, D-09111 Chemnitz, Germany*

Received March 5, 2010; Revised Manuscript Received April 20, 2010

ABSTRACT: Rod−coil copolymers with an oligomeric rod aggregate on a nanometer length scale, which is important for many applications like e.g. organic photovoltaics. However, this aggregation behavior and the driving forces such as hydrogen bonding and $\pi-\pi$ interactions, as well as the role of side groups, are not yet fully understood. Here, we investigated these noncovalent interactions in oligo(*p*-benzamide)−poly(ethylene glycol) (OPBA−PEG) copolymers using solid-state NMR supported by wide-angle X-ray scattering (WAXS), differential scanning calorimetry (DSC), and polarization optical microscopy (POM). It was found that longer OPBAs form layered β-sheet-like aggregates and that these are stabilized by amide hydrogen bonds in both unsubstituted OPBAs and OPBA−PEG rod−coil copolymers. The binding of the PEG also introduces a liquid crystalline phase. As a consequence, the local structural order is improved in the copolymer. Thus, by combining different methods of structural investigation, we were able to develop a model of local aggregation and packing in both the liquid crystalline and the solid state.

I. Introduction

Rod−coil block copolymers represent an interesting class of diblock copolymers due to their particular aggregation behavior. The interactions between various segments and geometric effects are responsible for nanoscaled phase separation and liquid crystallinity.[1−4] In particular, the ability to self-assemble on the nanometer length scale has promoted these systems for possible applications such as light-emitting diodes (LEDs) and organic photovoltaics[5−7] but also for the preparation of nanometer scaled architectures.[8,9]

The functionality of rod−coil block copolymers is mainly determined by well-defined structures and aggregation.[7] Understanding the driving force for their self-assembly is essential in order to control the tailored design of nanometer scaled materials. Therefore, rod−coil block copolymers with an oligomeric rod segment are of particular interest because their aggregation might depend on the respective length of the building blocks.

Here, we investigate copolymers built of oligomeric rod blocks of oligo(*p*-benzamides) (OPBA) and a poly(ethylene glycol) (PEG) coil (see Figure 1). An interesting feature of solid OPBAs is their rigidity resulting from packing due to hydrogen-bonding and $\pi-\pi$ interactions. Both are noncovalent interactions, and their influence on the structure of the studied system is not yet fully understood. Although the synthesis and analytical characterization of OPBAs are rather complex due to poor solubility and crystallization behavior, the synthesis of well-defined rod segments is feasible.[10−13]

Insight into aggregation and local packing of both OPBAs and OPBA-based rod−coil copolymers can be obtained from advanced high-resolution solid-state NMR, which is a powerful and versatile tool for the characterization of such materials.[14] In particular, solid-state NMR facilitates site-selective and noninvasive investigation of noncovalent interactions such as hydrogen-bonding and $\pi-\pi$ interactions. Signals originating from hydrogen-bonded protons are well separated in the ^{1}H magic-angle spinning (MAS) NMR spectrum, typically resonating between 8 and 20 ppm.[15−17] The ^{1}H chemical shift includes semiquantitative information about the strength of the hydrogen bonds.[18−20] In addition, the ^{1}H chemical shift is also a sensitive probe with respect to ring currents associated with aromatic moieties.[21,22] This is observed as a low field shift of the chemical shift compared to the corresponding liquid state signal and may thereby serve as a direct hint for $\pi-\pi$ interactions and can likewise be simply related to the packing via so-called nucleus independent chemical shift (NICS) maps.[14,23,24]

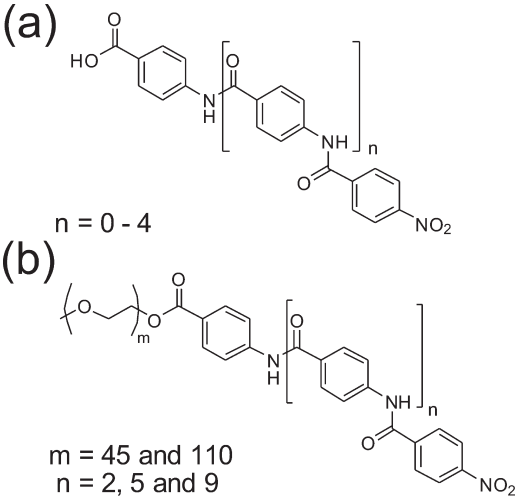

Figure 1. (a) Schematic overview of unsubstituted OPBAs with n = 0−4 repeat units named as OPBA-2 to OPBA-6 and (b) the investigated rod−coil copolymers with variation of rod and coil length (OPBA-7-PEG110, OPBA-11-PEG110, and OPBA-4-PEG45).

*To whom correspondence should be addressed.

 Published on Web 05/03/2010

Detailed insight about the local structure can be obtained from $^1H-^1H$ double-quantum single-quantum (DQ-SQ) correlation spectrum.[14,22] Such a 2D experiment correlates DQ coherence due to pairs of dipolar coupled protons with SQ coherence in characteristic correlation peaks. Diagonal peaks result from so-called like spins with the same chemical shift and cross peaks reflect couplings among unlike spins with different chemical shifts.

Information about the presence of polymorphs, local conformations, secondary structure motifs, and moieties comprising the asymmetric unit of powdered samples can be obtained by ^{13}C cross-polarization (CP) MAS measurements. Moreover, the ^{13}C line shapes include hints of structural order: broad lines indicate an ill-defined or possibly amorphous structure whereas narrow lines indicate crystallinity or high local order.[25−27]

To link the above-described methods, 2D $^{13}C/^1H$ correlation can be done which provide additional tools for studying local molecular assemblies and dynamics. Often applied NMR techniques are based on rotational echo double resonance (REDOR) for reintroducing the otherwise averaged heteronuclear dipolar coupling.[28] Specifically, the recoupled polarization transfer (REPT) technique allows recording of $^{13}C/^1H$ chemical shift correlation spectra and the determination of $^{13}C/^1H$ dipolar coupling constants by means of spinning sideband analysis in the indirect dimension of the 2D experiment.[29] In a recoupled polarization-transfer heteronuclear single quantum correlation (REPT-HSQC) experiment, the $^{13}C/^1H$ resonances are correlated in a two-dimensional fashion where the recoupling condition can be chosen such that either short- or long-range $^{13}C-^1H$ interactions are observed.[30] In contrast, the recoupled polarization-transfer heteronuclear dipolar order (REPT-HDOR) experiment does not correlate the chemical shifts of ^1H and ^{13}C, but the $^{13}C-^1H$ dipolar coupling.[31] Thus, REPT-HDOR is particular promising for the study of molecular dynamics where the reduction of heteronuclear dipolar coupling due to fast motional averaging can be investigated in a quantitative fashion.[32,33]

This paper is organized as follows. First, the aggregation behavior of unsubstituted OPBAs of different length is clarified by solid-state NMR, augmented by wide-angle X-ray scattering (WAXS). Second, the aggregation and site-specific local dynamics is investigated in rod−coil copolymers with varying rod length as well as different molar mass of the PEG block. Finally, the phase behavior of the rod−coil copolymers is clarified by differential scanning calorimetry (DSC), solid-state NMR, and optical microscopy, and the impact of the liquid crystalline phase on the local order of the aggregate in the solid is considered.

II. Experimental Methods

Samples Preparation. The syntheses of OPBA-2, OPBA-3, and OPBA-4 as well as the rod−coil copolymers OPBA-4-PEG45 and OPBA-7-PEG110 were carried out as described previously.[10] 4-((*Z*)-Chloro(4-((*Z*)-chloro(4-nitrophenyl)methyleneamino)-phenyl)methyleneamino)benzoyl chloride (compound **6** in ref 10) will be referred to as imidoyl chloride trimer precursor. The amine-terminated block copolymer corresponding to OPBA-7-PEG110 (i.e., where the nitro group is reduced to a primary amine) will be referred to as NH_2-OPBA-7-PEG110. The reduction of OPBA-7-PEG110 to the amine-terminated polymer was carried out in analogy to the previously reported procedures for shorter OPBA−PEG block copolymers.[10]

4-(4-(4-Aminobenzamido)benzamido)benzoic Acid. 4-(4-(4-Nitrobenzamido)benzamido)benzoic acid (10 g, 25 mmol) was dissolved in a mixture of methanol (300 mL) and DMF (50 mL). Ammonium formate (15 g, 250 mmol) was added to the stirred solution. Pd/C (10%, 1 g) was subsequently added in small portions under a nitrogen atmosphere. After stirring for 12 h at room temperature (rt) the mixture was filtered through Celite (Aldrich), and the solvents were removed under reduced pressure. HCl(conc) was added to the residue, and the white precipitate was recovered by filtration. The solid was washed with water until the pH of the filtrate was neutral and then dried under high vacuum to yield the title compound in 86% (8 g, 0.21 mol). ^1H NMR (DMSO-d_6): δ (ppm) = 5.83 (bs, $-NH_2$), 6.62 (d, 6.64 Hz, 2 H, ar), 7.75 (d, 6.64 Hz, 2 H), 7.90 (m, 8 H), 10.05 (s, 1 H, −NH), 10.40 (s, 1 H, −NH). MS (FD): *m*/*z* (%): 375.1 (100), 376.1 (21.99), 377.1 (2.99); calcd 375.12 (100), 376.13 (23.8), 377.13 (3.5), 376.12 (1.1).

OPBA-5. 4-(4-Aminobenzamido)benzoic acid (10 g, 37 mmol) was dissolved in NMP (80 mL) and added to a stirred solution of imidoyl chloride trimer precursor (17 g, 37 mmol) and *N,N′*-dimethyl aniline (37 mmol) in NMP (80 mL) at rt. After stirring at rt for 12 h the mixture was poured into HCl (0.1 N), and the precipitated solid was removed by filtration. The solid was washed with water until the filtrated was at neutral pH. The solid was dried under vacuum and subsequently washed with diethyl ether. The solid was then extracted with NMP in a Soxhlet extractor for 12 h to remove all soluble impurities of the starting materials. The solid was dried under high vacuum, yielding 23 g of a light yellow solid.

OPBA-6. 4-(4-(4-Aminobenzamido)benzamido)benzoic acid (2 g, 5.3 mmol) was dissolved in NMP (10 mL) and added to a stirred solution of imidoyl chloride trimer precursor (2.5 g, 5.4 mmol) and *N,N′*-dimethylaniline (5.4 mmol) in NMP (10 mL) at rt. After stirring at rt for 12 h the mixture was poured into HCl (0.1 N), and the precipitated solid was removed by filtration. The solid was washed with water until the filtrate was at neutral pH. The solid was dried under vacuum and subsequently washed with diethyl ether. The solid was then extracted with NMP in a Soxhlet extractor for 12 h to remove all soluble impurities of the starting materials. The solid was dried under high vacuum, yielding 4 g of a light yellow solid.

OPBA-11-PEG110. Imidoyl chloride trimer precursor (580 mg, 1.3 mmol) was added to a solution of NH2-OPBA-7-PEG110 (1.5 g, 0.25 mmol) and *N,N′*-dimethylaniline (160 μL) in DMF (10 mL). After stirring at rt for 24 h the polymer was precipitated into a 10-fold excess of diethyl ether, and the solid was recovered by filtration. Drying under high vacuum yielded the title compound.

Solid-State NMR Spectroscopy. All ^1H MAS NMR spectra were measured at a Bruker Avance 700 MHz spectrometer using 30 kHz MAS and a $\pi/2$ pulse of 2.5 μs. The recycle delay was 60 s for unsubstituted OPBAs and 5 s for the copolymers. $^1H-^1H$ DQ-SQ MAS NMR were also performed at 700 MHz at 30 kHz MAS and a $\pi/2$ pulse of 2.5 μs. The back-to-back (BABA) recoupling sequence was used applying States-TPPI for phase sensitive detection.[34] The recycle delay was 2 s, and for each of the 128 t_1-slices 32 transients were recorded. ^{13}C CP/MAS measurements were carried out at 125.77 MHz (Bruker Avance 500 machine) using 25 kHz MAS and a $\pi/2$ pulse of 2.5 μs. Spectra were measured with a CP contact time of 3 ms, 4096 scans, a recycle delay of 15 s, and TPPM decoupling.[35] REPT-HSQC experiments[30] were carried out using a Bruker Avance-III 850 spectrometer with a ^{13}C resonance of 213 MHz and a $\pi/2$ pulse of 2.5 μs. The measurement was acquired with 2 rotor periods recoupling, 72 increments in the indirect dimension, 1024 transients per increment, and a recycle delay of 2 s. REPT-HDOR measurements[31] were performed using a Bruker Avance 500 spectrometer at 25 kHz MAS and a $\pi/2$ pulse of 2.5 μs. The experiment was measured employing 4 rotor periods recoupling, 20 increments in the indirect dimension, 1120 transients per increment, and a recycle delay of 2 s. For analyzing the data a home written Matlab routine was used which is based on the dipolar coupling of a two-spin system.[29] All ^1H and ^{13}C MAS NMR spectra were referenced with respect to tetramethylsilane (TMS) using solid tetrakis(trimethylsilyl)silane (TTSS) and solid adamantane as a secondary standard.[36,37]

POM observations were made with a Zeiss Axioscop 40 equipped with a Linkam THMS600 hot stage.

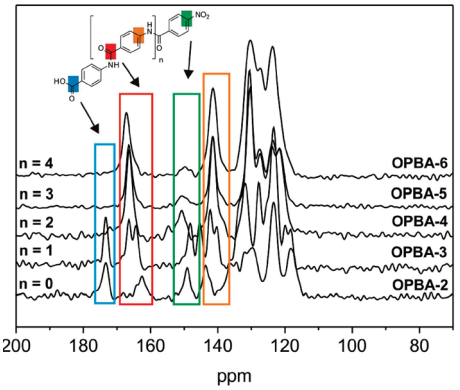

Figure 2. ^{13}C CP/MAS spectra of OPBAs with increasing number of repeat units. Resonance assignment is clarified by the color code. It is shown that for OPBA-4 (n = 2) and the longer OPBAs all spectra are rather similar, indicating an equilibrium structure.

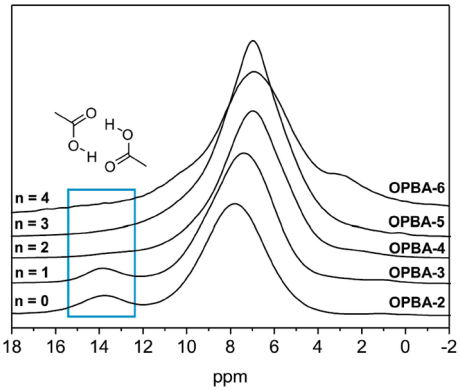

Figure 3. ^{1}H MAS NMR spectra of OPBA-2 to OPBA-6. The inset illustrates the hydrogen bond formation through an acid dimer (resonance at 14 ppm present in OPBA-2 and -3) The spectrum of OPBA-6 (n = 4) shows additional signals due to impurities since the solubility is rather poor and the purification difficult.[10]

Wide-angle X-ray scattering measurements were carried out with a D8 Advanced Bruker on powder samples on a glass substrate.

III. Results and Discussion

Unsubstituted OPBAs. First, the dependence of aggregation on the length of the oligomer was studied in unsubstituted OPBAs. Particularly suited for this kind of investigation is the ^{13}C CP/MAS experiment which is sensitive to structural changes and local degree of organization (spectra shown in Figure 2). The resonance at 172 ppm is assigned to the COOH group, while the CONH carbon has a chemical shift of about 164 ppm and the signals at about 150 and 142 ppm can be assigned to the quaternary carbon atoms bearing nitro- and amide groups (see color code Figure 2). The signals in the region of 120−140 ppm can be assigned to the aromatic carbon atoms.[38]

Comparison of the ^{13}C CP/MAS spectra show that the spectra of OPBA-2 and -3 differ as compared to those of OPBA-4 to -6. This indicates that the structure for the short OPBAs with n = 0 and 1 is different from that of the longer oligomers. In particular, the well-resolved peak at 172 ppm of the COOH group is only present in OPBA-2 and -3. Remarkably, longer OPBAs with four and more repeat units ($n \geq 2$) have rather similar ^{13}C spectra, suggesting an equilibrium structure (see Figure 2). The only observable difference for the longer OPBAs is a noticeable degradation of the spectral resolution, probably due to decreasing crystallinity of the samples.

The ^{1}H MAS NMR spectra (shown in Figure 3) also reflect this behavior. For OPBA-2 and -3 a strong peak at about 14 ppm is observed that can be assigned to the hydrogen bonding of two carboxylic acid groups forming a dimer (see inset Figure 3).[39] The absence of this signal for longer OPBAs indicates that these are not able to form hydrogen bonds between carboxylic acid groups, which also explains the absence of the peak at 172 ppm in the ^{13}C CP/MAS spectra. Because of the lack of hydrogen bonding the chemical shift of the carboxylic acid carbon atom is shifted toward higher field and thus overlaps with the chemical shift of the CONH peak at 164 ppm. All ^{1}H MAS NMR spectra include a broad peak at about 7 ppm which can be assigned to the aromatic protons. The resonance for the amide protons of the peptide bond is located at about 9 ppm and hidden below the broad aromatic signal, as demonstrated by deuterium exchange and subsequent ^{2}H MAS NMR measurements.[40] The spectrum of OPBA-6 (n = 4) shows additional signals due to impurities since the solubility of the longer OPBAs is rather poor and the purification difficult.[10]

Obviously, the rod length affects what kind of hydrogen bonding determines the structure. On the one hand, the hydrogen bonding of two carboxylic acid groups is known to be rather strong compared to the much weaker amide hydrogen bonds.[41] But on the other hand, the number of amide hydrogen bonds is increasing with increasing rod size, whereas the formation of the carboxylic dimers is limited to the end groups. For OPBA-2 and -3, the ratio of the two types of hydrogen bonding is 1:1 and 1:2, respectively, and therefore the carboxylic acid dimer formation is facilitated. Both structures including the hydrogen-bonding network have already been discussed in detail in a previous paper.[40] With increasing number of repeat units the ratio of the carboxylic acid hydrogen bond formation compared to the amide hydrogen bond formation decreases. The amide hydrogen bonding dominates the structure formation for the longer oligomers, starting with OPBA-4, as shown by the absence of the peaks at 14 ppm in the ^{1}H MAS NMR spectrum and 172 ppm in the ^{13}C CP/MAS NMR spectrum.

To further reveal the impact of hydrogen bonding on the structure, the influence of a hydrogen bond breaking solvent was probed upon crystallization of OPBA-3 with dimethylformamide (yielding OPBA-3-DMF). The carboxylic acid end groups are blocked by DMF, and almost no dimer formation is observed as for OPBAs with $n \geq 2$. Comparison of the ^{13}C CP/MAS NMR spectra of OPBA-3-DMF and OPBA-5 (shown in Figure 4) indicates that both spectra match, apart from the presence of a minority component with carboxylic dimers as indicated by the ^{13}C signal at 172 ppm. All signals in the ^{13}C CP/MAS NMR spectrum have rather similar chemical shifts. An important difference however is the spectral resolution due to the fact that OPBA-3-DMF forms a regular crystal lattice whereas OPBA-5 does not. Therefore, the ^{13}C CP/MAS NMR spectrum of OPBA-3-DMF was also processed with an additional line broadening of 150 Hz (see Figure 4b), obscuring fine splitting. This underlines the similarity of both spectra and, hence, indicates a comparable solid-state packing.

As an independent probe, wide-angle X-ray scattering (WAXS) of both OPBA-3-DMF and OPBA-5 was performed (shown in Figure 5). The wide angle range ($2\theta > 15°$) reflects the local structure comparable to the data available by solid-state NMR. There are three main reflexes at 2θ = 20.3 (h, k, l: −2, 1, 3), 2θ = 23.7 (h, k, l: −4, 0, 4), and 2θ = 27.8 (h, k, l: −3, 1, 5) which match for OPBA-3-DMF

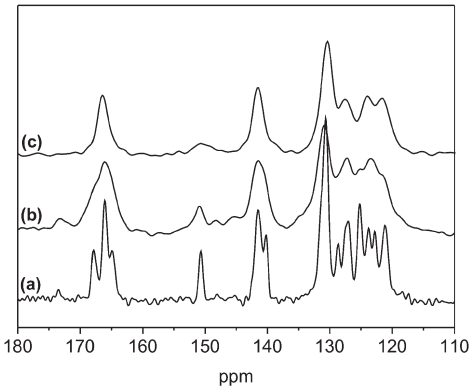

Figure 4. ^{13}C CP/MAS NMR spectrum of (a) OPBA-3-DMF and (b) OPBA-3-DMF processed with an additional line broadening of 150 Hz and (c) OPBA-5. Especially the comparison of (b) and (c) shows that both spectra match almost perfectly.

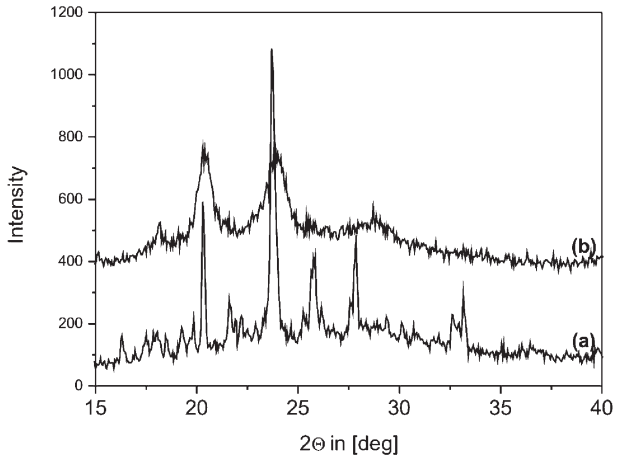

Figure 5. WAXS pattern of (a) OPBA-3-DMF and (b) OPBA-5 which underlines the structural similarity.

and OPBA-5 rather well. Similar to the NMR data, the match of the main reflexes underlines the structural similarity. The single-crystal X-ray structure of OPBA-3-DMF exhibits a hydrogen-bonded stack of rods.[8] On the basis of that observation, the structural features must also be present in the longer OPBAs. Thus, it is expected that longer OPBAs form a regularly layered β-sheet-like hydrogen-bonded structure with no linkage of the head groups (see Figure 6a). Moreover $\pi-\pi$ stacking interactions are present between the layers (see Figure 6b).

Rod−Coil Copolymers. Bonding the rod to PEG polymers yields rod−coil copolymers. Potential structural changes can then be monitored in the corresponding ^{13}C CP/MAS NMR spectrum (shown in Figure 7). The signals attributed to the OPBA rod within the copolymer appear in the same region of 110−165 ppm as in unsubstituted OPBAs. Comparison of the ^{13}C signals shows a good match between the unsubstituted OPBAs and the OPBA rods incorporated in the polymer (shown in Figure 7a). The additional signal at 70 ppm reflects the PEG coil. Since the coil length may influence the structure, a comparison of the ^{13}C CP/MAS NMR spectra of OPBA-7-PEG110 and OPBA-4-PEG45 is shown in Figure 7b. Although the length of the PEG coil has more than doubled, the ^{13}C CP/MAS NMR spectrum has not changed. The same consistency of the ^{13}C signals is observed upon changing the rod length (see in Figure 7c), indicating that the rod structure is unchanged under these circumstances.

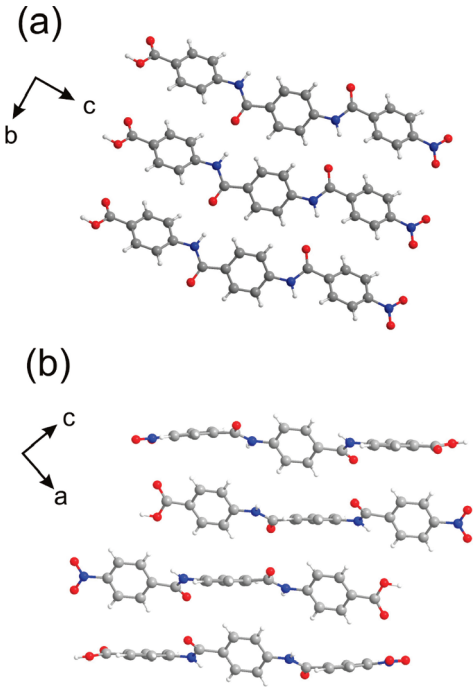

Figure 6. Projections of the OPBA-3-DMF single crystal X-ray structure with the unit cell dimension of a = 24.5 Å, b = 5.4 Å, c = 17.1 Å, and β = 99.05°.[8] (a) Amide hydrogen bonding within a layer and the formation of a β-sheet-like structure; (b) stacking between the layers.

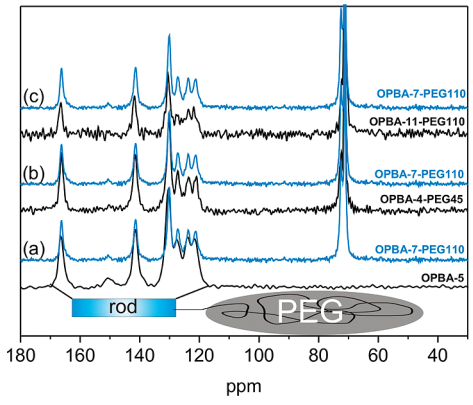

Figure 7. ^{13}C CP/MAS NMR spectra of (a) OPBA-5 (black) and OPBA-7-PEG110 (blue), (b) OPBA-4-PEG45 (black) and OPBA-7-PEG110 (blue), and (c) OPBA-11-PEG110 (black) and OPBA-7-PEG110 (blue). Concerning the consistency of the ^{13}C signals, it can be concluded that the structure of OPBAs remains although a PEG coil is attached. The rod structure is also unaffected by variation of the coil and rod length.

On the basis of the observation that the structure of OPBAs with $n \geq 2$ is very similar to the structure of OPBA-3-DMF and the structure of OPBA rods within the copolymer reflects that of the unsubstituted OPBAs, we propose a tentative packing of the rod−coil copolymer as depicted in Figure 8. Within a layer there is a β-sheet-like hydrogen-bonding network where all PEG chains are oriented in the same direction. Between the layers $\pi-\pi$ stacking interactions are present and the polymer chains are oriented in an alternate way. The volume filled by the attached PEG polymer chains is described by an elongated sphere of different sizes, depending on the length of the specific PEG.[42] At first sight, the fact that the oligomers are oriented in the same direction within one layer might

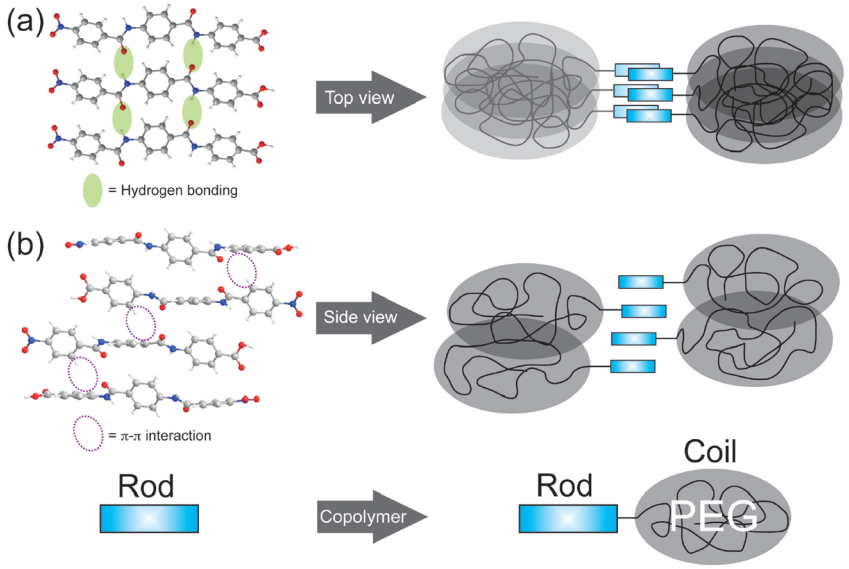

Figure 8. Schematic structure of the rod coil copolymer. The rod block is depicted with a blue box and the PEG coil with a gray ellipse. (a) shows the idea of aggregation within a layer and the driving forces of hydrogen bonding and (b) the aggregation between the layers with the driving forces of $\pi-\pi$ interactions.

raise the question how such a packing could lead to a proper space filling structure. In similar rigid rod systems with alkyl side chains of different lengths it has been observed that the flexibility of these chains allows for a dense packing imposed by the rigid rods.[43] In the present case of OPBA with attached PEG chains this will be even easier since such chains are know to be more flexible.[42] It is also reasonable to assume that the arrangement of OPBA−PEG copolymers is very similar, or identical, to micelles formed in solution and in the solid state. The observations made here, however, are in contrast to the previous sketch of molecular arrangement that OPBA rods form a bilayer within the core of the "hockey-puck micelles".[8] The molecular arrangement was derived from topography images obtained by scanning force microscopy (SFM). While SFM can give very accurate height dimensions, the finite size of the scanning tip itself limits the accuracy of objects laterally. Therefore, the tip geometry must be considered in the interpretation of SFM data. Considering this and analyzing the SFM phase contrast images, the existence of bilayer hockey-puck micelle is very unlikely. With the current solid-state NMR data, it can be assumed that the geometric arrangement as depicted in Figure 8 is the most likely description of the arrangement of the OPBA rod blocks within the micellar core. To underline this property, the packing of OPBA-7-PEG110 has been analyzed via 2D $^{1}H-^{1}H$ DQ-SQ MAS NMR and $^{13}C/^{1}H$ REPT-HSQC NMR.

The 2D $^{1}H-^{1}H$ DQ-SQ MAS NMR spectrum of OPBA-7-PEG110 shown in Figure 9a was recorded at low temperature (250 K) in order to shrink the intense PEG signal. In the projection, besides the signal at 3.8 ppm (resonance D) assigned to PEG, three additional resonances at 9.1 ppm (resonance A), 7 ppm (resonance B), and 5.5 ppm (resonance C) are observed. The signal at 9.1 ppm can be assigned to the amide protons which are directly observable at that temperature. The remaining two peaks at 7 and 5.5 ppm originate from the aromatic protons, where the chemical shift of 5.5 ppm indicates $\pi-\pi$ stacking present in the system (protons are marked in red, see chemical structure in Figure 9a).[19] The correlation among protons participating in different local packing can be identified via characteristic cross-peaks in the 2D spectrum. The DQ cross-peak at 12.5 ppm (resonance BC 7 ppm + 5.5 ppm) indicates contacts among aromatic protons with and without $\pi-\pi$ stacking. The DQ auto-peak at 14 ppm (resonance BB 7 ppm + 7 ppm) indicates contacts among aromatic protons, while the DQ cross-peak at 16.1 ppm (resonance AB 9.1 ppm + 7 ppm) reflects proximity of aromatic protons and amide protons. Additional insights into the local packing is derived from $^{13}C/^{1}H$ REPT-HSQC NMR (shown in Figure 9b). The peak assignment is pointed out by the color code shown in Figure 9b. It can be noticed that not only the proton chemical shift is affected by $\pi-\pi$ stacking interactions but also the ^{13}C chemical shift.[21] Both 2D measurements underline the aggregation behavior derived from the single-crystal X-ray structure.

Phase Behavior of Rod−Coil Copolymers. Beside all structural similarities discussed above, it should be noticed that the resolution in the ^{13}C/CP MAS spectrum of the copolymer is significantly increased compared to the corresponding unsubstituted OPBAs (cf. ^{13}C/CP MAS spectra of OPBA-6 and OPBA-7-PEG110 in Figure 10). In principle, there are two possibilities for an increased resolution of a ^{13}C CP/MAS solid-state NMR spectrum: either the mobility or the local order of the OPBA rod incorporated in the copolymer has increased. To clarify this question, the mobility of the rod segment is analyzed via the $^{13}C/^{1}H$ REPT-HDOR method. The aromatic ^{13}C resonance at 123 ppm was chosen for detecting the dipolar sideband pattern and subsequent fitting to obtain the $^{13}C/^{1}H$ dipolar coupling constant (see fitted sideband pattern Figure 11).[33] For both OPBA-7-PEG110 and OPBA-5, the measured $^{13}C-^{1}H$ dipolar coupling constant is 18.0 ± 0.5 kHz, indicating that the aromatic rings are rather rigid (for a completely rigid system 21.0 kHz is expected). The almost identical $^{13}C-^{1}H$ dipolar coupling constant also shows that the mobility of the OPBA rod is unaffected by PEG attachment. Thus, the increased spectral resolution in the ^{13}C/CP MAS spectrum stems from a higher local order of the rod structure.

Apart from phase separation and aggregation, another important characteristics of rod−coil copolymers is their ability to form liquid crystalline phases.[2,4,44] Of special importance are lamellar and nematic phases. For model

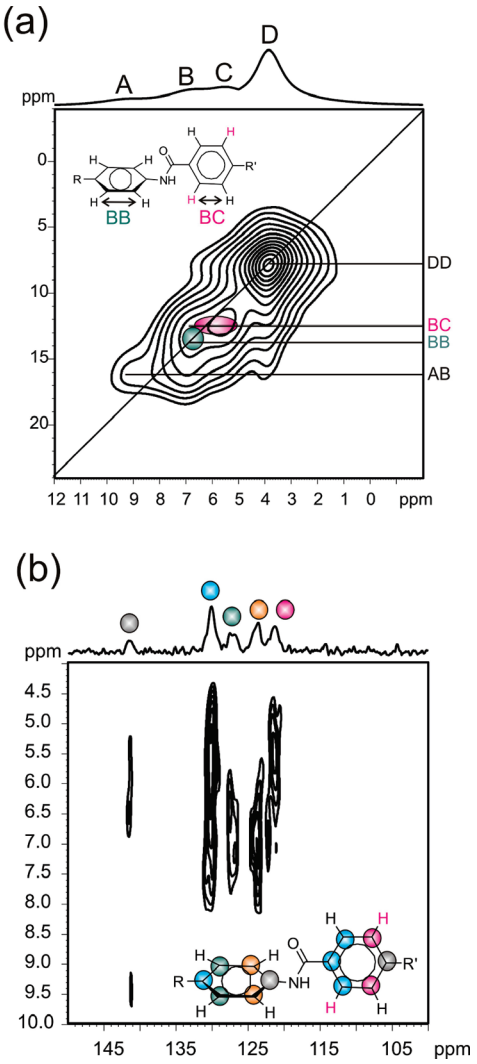

Figure 9. (a) 2D $^{1}H-^{1}H$ DQ-SQ MAS NMR spectrum of OPBA-7-PEG110 performed at 250 K and 30 kHz MAS with $1\tau_R$ recoupling. (b) 2D $^{13}C-^{1}H$ REPT-HSQC spectrum of OPBA-7-PEG110 measured at 25 kHz MAS and $2\tau_R$ recoupling.

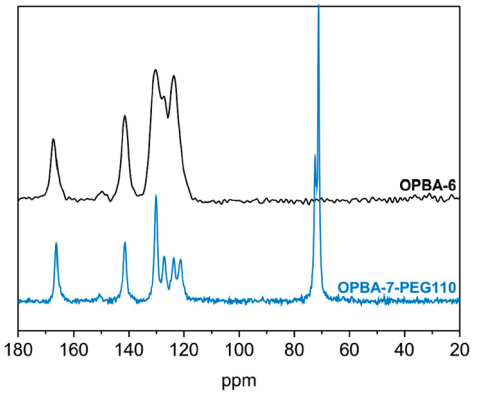

Figure 10. ^{13}C CP/MAS NMR spectrum of OPBA-6 (black) and OPBA-7-PEG110 (blue). The aromatic signals in case of the copolymer are much better resolved, although the rod part includes more repeat units.

systems also complete phase diagrams are reported. Depending on the asymmetry between the rod and coil also a hexagonal packed phase was observed.[45]

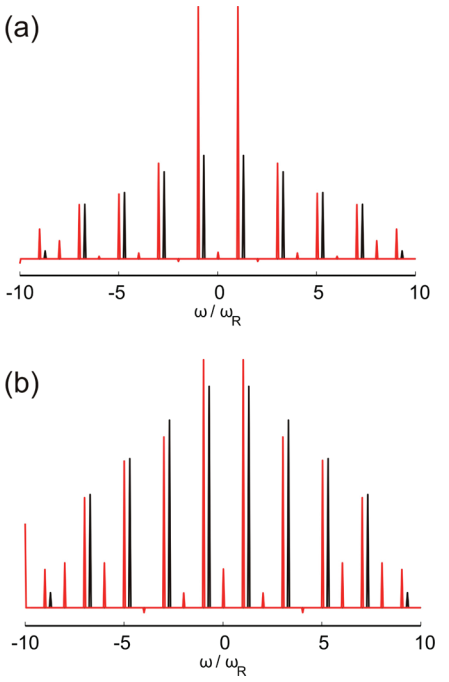

Figure 11. $^{13}C-^{1}H$ REPT-HDOR spinning sideband pattern of (a) OPBA-5 and (b) OPBA-7-PEG110. The measurement was performed at 25 kHz MAS and 4 rotor periods recoupling. The red spectra correspond to the measured $^{13}C-^{1}H$ dipolar spinning sideband pattern, and the black spectra are the fitting curves. Multispin interactions affect the innermost dipolar sidebands in (a), and therefore the fifth and seventh sidebands were chosen to evaluate the goodness of the fit. The determined $^{13}C-^{1}H$ dipolar coupling constant is in both cases 18 kHz.

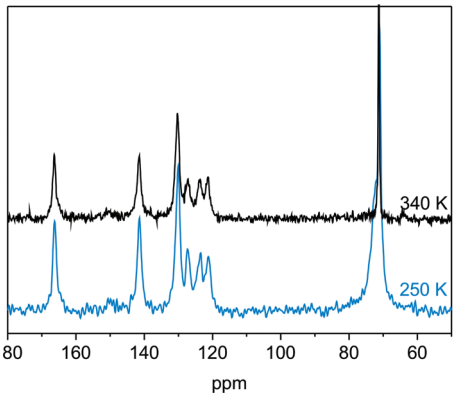

Figure 12. ^{13}C CP/MAS NMR spectra of OPBA-7-PEG110 recorded at 250 K (black) and 340 K (blue). The OPBA signals (120−165 ppm) are hardly influenced by temperature changes while the PEG signal at 71 ppm shows a significant decrease of the line width (from 130 Hz at 250 K to 50 Hz at 340 K), indicating a higher mobility.

Indeed for OPBA-7-PEG110 the DSC trace shows an exothermic peak at 332 K, in agreement with the recent studies of the melting temperature of a similar rod−coil copolymer at 329 K.[11] To investigate how the nature of this transition affects the structure, VT-^{13}C CP/MAS measurements in the temperature range up to 340 K were performed to monitor possible changes of the structure. Since the ^{13}C resonances in the ^{13}C/CP MAS spectrum attributed to the rod (120−165 ppm) are well separated from those of the coil (71 ppm), structural changes can be observed individually. Figure 12 shows the ^{13}C CP/MAS NMR spectra recorded at specific temperatures of 250 and 340 K, i.e., well below and slightly above the phase transition. While OPBA signals in

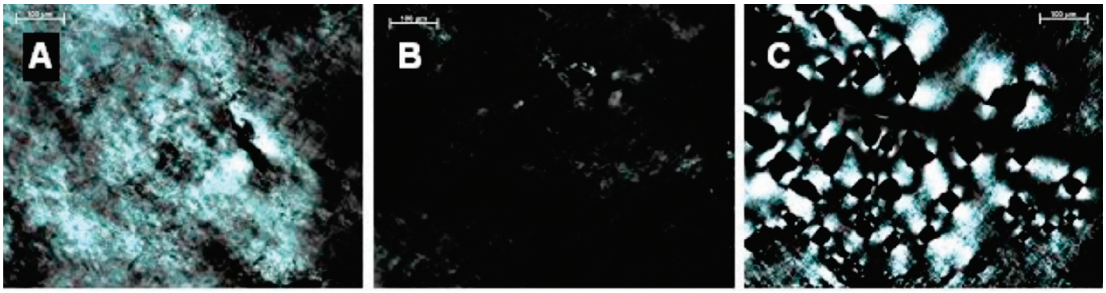

Figure 13. POM of OPBA-4-PEG45 images at 105 °C. (A) and (B) show a certain position of the sample but rotated by 45°. (C) Birefringent nonspecific texture.

the range of 120−160 ppm exhibit almost no changes, the PEG signal at 71 ppm narrows substantially above 332 K. Thus, the phase transition detected by DSC reflects melting of the PEG block only. This is in accord with the statement in the literature that the rodlike character is retained under virtually all circumstances.[2]

Probing the formation of a liquid crystalline phase with a polarization optical microscope (POM) is presented in Figure 13, and these indeed show that above the melting temperature a liquid crystalline phase is formed for all the examined rod−coil copolymers. Rotation of the samples exhibited alternately birefringent and dark textures every 45° (shown in Figure 13A,B). The nonspecific textures can be sheered but have not been assigned to a certain kind of mesophase. It is known that the presence of a liquid crystalline phase favors supramolecular organization when cooling down to a solid phase.[33,46] Thus, the better local order of the aggregation in the rod−coil copolymer noted above is likely to be due to the preorganization in the liquid crystalline phase.

IV. Conclusion

The structures of both unsubstituted OPBAs and OPBA−PEG rod−coil copolymers have been investigated by solid-state NMR, WAXS, DSC, and POM. It was found that longer OPBAs form hydrogen-bonded layered β-sheet-like aggregates, which are remarkably stable and apparently reflect an equilibrium structure. This equilibrium structure is retained after PEG attachment forming a rod−coil copolymer. At elevated temperatures a transition to a liquid crystalline phase of the rod−coil copolymer is observed by DSC, and from solid-state NMR this has been ascribed to melting of the PEG coil, where the aggregates of the OPBA rods are preserved. Because of the preorganization in the liquid crystalline phase, an improvement of the local order is observed for the OPBA rod in the copolymer.

Acknowledgment. We thank Verona Maus und Michelle Drechsler for measuring DSC and the Deutsche Forschungsgemeinschaft (SFB 625) for financial support.

Note Added after ASAP Publication. This paper was published on the Web on May 3, 2010, with the incorrect artwork for Figure 12. The corrected version was reposted on May 5, 2010.

References and Notes

(1) Lee, M.; Cho, B.-K.; Zin, W.-C. *Chem. Rev.* **2001**, *101*, 3869–3892.
(2) Klok, H.-A.; Langenwalter, J. F.; Lecommandoux, S. *Macromolecules* **2000**, *33*, 7819–7826.
(3) Olsen, B. D.; Segalman, R. A. *Macromolecules* **2005**, *38*, 10127–10137.
(4) Olsen, B. D.; Segalman, R. A. *Macromolecules* **2006**, *39*, 7078–7083.
(5) Segalman, R. A.; McCulloch, B.; Kirmayer, S.; Urban, J. J. *Macromolecules* **2009**, *42*, 9205–9216.
(6) Osaheni, J. A.; Jenekhe, S. A. *J. Am. Chem. Soc.* **1995**, *117*, 7389–7398.
(7) de Boer, B.; Stalmach, U.; van Hutten, P. F.; Melzer, C.; Krasnikov, V. V.; Hadziioannou, G. *Polymer* **2001**, *42*, 9097–9109.
(8) Schleuss, T. W.; Abbel, R.; Gross, M.; Schollmeyer, D.; Frey, H.; Maskos, M.; Berger, R.; Kilbinger, A. F. M. *Angew. Chem., Int. Ed.* **2006**, *45*, 2969–2975.
(9) König, H. M.; Kilbinger, A. F. M. *Angew. Chem., Int. Ed.* **2007**, *46*, 8334–8340.
(10) Abbel, R.; Frey, H.; Schollmeyer, D.; Kilbinger, A. F. M. *Chem.—Eur. J.* **2005**, *11*, 2170–2176.
(11) Abbel, R.; Schleuss, T. W.; Frey, H.; Kilbinger, A. F. M. *Macromol. Chem. Phys.* **2005**, *206*, 2067–2074.
(12) König, H. M.; Gorelik, T.; Kolb, U.; Kilbinger, A. F. M. *J. Am. Chem. Soc.* **2007**, *129*, 704–708.
(13) Gabellini, A.; Novi, M.; Ciferri, A.; Dell'Erba, C. *Acta Polym.* **1999**, *50*, 127–134.
(14) Brown, S. P.; Spiess, H. W. *Chem. Rev.* **2001**, *101*, 4125–4155.
(15) Chierotti, M. R.; Gobetto, R. *Chem. Commun.* **2008**, *14*, 1621–1634.
(16) Emmler, T.; Gieschler, S.; Limbach, H. H.; Buntkowsky, G. *J. Mol. Struct.* **2004**, *700*, 29–38.
(17) Brunner, E.; Sternberg, U. *Prog. Nucl. Magn. Reson. Spectrosc.* **1998**, *32*, 21–57.
(18) Yamauchi, K.; Kuroki, S.; Fujii, K.; Ando, I. *Chem. Phys. Lett.* **2000**, *324*, 435–439.
(19) Schmidt, J.; Hoffmann, A.; Spiess, H. W.; Sebastiani, D. *J. Phys. Chem. B* **2006**, *110*, 23204–23210.
(20) Gu, Z. T.; Redenour, C. F.; Bronnimann, C. E.; Iwashita, T.; McDermott, A. *J. Am. Chem. Soc.* **1996**, *118*, 822–829.
(21) Lazzeretti, P. *Prog. Nucl. Magn. Reson. Spectrosc.* **2000**, *36*, 1–88.
(22) Brown, S. P. *Prog. Nucl. Magn. Reson. Spectrosc.* **2007**, *50*, 199–251.
(23) Brown, S. P.; Schnell, I. S.; Brand, D.; Müllen, K.; Spiess, H. W. *J. Am. Chem. Soc.* **1999**, *121*, 6712–6718.
(24) Sebastiani, D. *ChemPhysChem.* **2006**, *7*, 164–175.
(25) Harris, R. K. *Analyst* **2006**, *131*, 351–373.
(26) Harris, R. K. *Solid-State Sci.* **2004**, *6*, 1025–1037.
(27) Gitsas, A.; Floudas, G.; Mondeshki, M.; Spiess, H. W.; Aliferis, T.; Iatrou, H.; Hadjichristidis, N. *Macromolecules* **2008**, *41*, 8072–8080.
(28) Gullion, T. *Magn. Reson. Rev.* **1997**, *17*, 83–131.
(29) Saalwächter, K.; Schnell, I. *Solid State Nucl. Magn. Reson.* **2002**, *22*, 154–187.
(30) Saalwächter, K.; Graf, R.; Spiess, H. W. *J. Magn. Reson.* **1999**, *140*, 471–476.
(31) Paul, S. M. D.; Saalwächter, K.; Graf, R.; Spiess, H. W. *J. Magn. Reson.* **2000**, *146*, 140–156.
(32) Hentschel, R.; Sillescu, H.; Spiess, H. W. *Polymer* **1981**, *22*, 1516–1521.
(33) Hansen, M. R.; Schnitzler, T.; Pisula, W.; Graf, R.; Müllen, K.; Spiess, H. W. *Angew. Chem., Int. Ed.* **2009**, *48*, 4621–4624.
(34) Feike, M.; Demco, D. E.; Graf, R.; Gottwald, J.; Hafner, S.; Spiess, H. W. *J. Magn. Res. Ser. A* **1996**, *122*, 214–221.
(35) Bennett, A. E.; Rienstra, C. M.; Auger, M.; Lakshimi, K. V.; Griffin, R. G. *J. Chem. Phys.* **1995**, *103*, 6951–6958.
(36) Muntean, J. V.; Stock, L. M.; Botto, R. E. *J. Magn. Reson.* **1988**, *76*, 540–542.
(37) Morkombe, C. R.; Zilm, K. *J. Magn. Reson.* **2003**, *162*, 479–486.

(38) Cavallaro, S.; Cum, G.; Gallo, R.; Spadaro, A.; Visalli, G. *Magn. Reson. Chem.* **2002**, *40*, 219–224.
(39) Khan, M. K.; Brunklaus, G.; Enkelmann, V.; Spiess, H. W. *J. Am. Chem. Soc.* **2008**, *130*, 1741–1748.
(40) Gorelik, T.; Kolb, U.; Matveeva, G.; Schleu, T.; Kilbinger, A. F. M.; van de Streek, J.; Bohle, A.; Brunklaus, G. *CrystEngComm* **2010**, doi: 10.1039/B920569A.
(41) Steiner, T. *Angew. Chem., Int. Ed.* **2002**, *41*, 48–76.
(42) Lee, H.; de Vries, A. H.; Marrink, S.-J.; Pastor, R. W. *J. Chem. Phys. B* **2009**, *113*, 13186–13194.
(43) Adam, A.; Spiess, H. W. *Makromol. Chem., Rapid Commun.* **1990**, *11*, 249–259.
(44) Olsen, B. D.; Shah, M.; Ganesan, V.; Segalman, R. A. *Macromolecules* **2008**, *41*, 6809–6817.
(45) Olsen, B. D.; Segalman, R. A. *Macromolecules* **2007**, *40*, 6922–6929.
(46) Percec, V.; Glodde, M.; Bera, T. K.; Miura, y.; Shiyanovskaya, I.; Singer, K. D.; Balagu-rusamy, V. S. K.; Heiney, P. A.; Schnell, I.; Rapp, A.; Spiess, H. W.; Hudson, S. D.; Duan, H. *Nature* **2002**, *417*, 384–387.